Varied line spacing plane holographic grating recorded by using uniform line spacing plane gratings

Ling Qing, Wu Gang, Liu Bin, and Wang Qiuping

Uniform line spacing plane gratings are introduced into a recording system to generate aspherical wavefronts for recording varied line spacing plane holographic gratings. Analytical expressions of groove parameters are derived to the fourth order. A ray-tracing validation algorithm is provided based on Fermat's principle and a local search method. The recording parameters are optimized to record a varied line spacing plane holographic grating with the aid of derived analytical expressions. A design example demonstrates the exactness of the analytical expressions and the superiority of recording optics with auxiliary gratings. © 2006 Optical Society of America

OCIS codes: 050.1950, 220.2740.

1. Introduction

Holographic gratings are fabricated by recording the interference fringes of two light beams in a photoresist coating on grating blanks. Given the shape of blanks, their focal properties can be adjusted by altering the properties of the two recording sources. The interference of two plane wavefronts in plane blanks results in conventional gratings with uniform line spacing (ULS) and straight grooves. The interference of spherical wavefronts results in grating grooves with varied line spacing (VLS) and curved grooves. It adds a degree of freedom to eliminate certain types of aberrations.[1] Koike and Harada[2] and Duban[3] introduced aspherical wavefronts to the fabrication of holographic gratings. This method added a greater degree of freedom and produced more powerful aberration-corrected holographic gratings. Holographic gratings recorded with aspherical wavefronts are the trend in fabrication and will play an important role in high-resolution spectrometers and monochromators.

There are three main methods to generate aspherical wavefronts in holographic recording.

(i) The first method uses auxiliary mirrors. Namioka and Koike[4] derived analytical expressions of groove parameters to the fourth order for the recording system that uses two ellipsoidal mirrors to generate aspherical wavefronts and an ellipsoidal blank as the grating blank. This type of holographic grating has been widely used in spectrographs and monochromators.[5–8] One of the disadvantages of this mounting is that it is sensitive to the tolerances of distance parameters and angle parameters in the recording optics.[9]

(ii) The second method uses multimode deformable mirrors (MDMs). Duban studied the theory,[10,11] discussed the realization,[12] and simulated the performance in the cosmic origins spectrograph (COS) gratings.[13,14] The main difficulty of this mounting comes from the fabrication of the MDMs.

(iii) The third method uses auxiliary gratings. Duban[15,16] investigated the holographic Rowland mounting, which consists of a Rowland-mounted and optimally recorded holographic spherical grating, referred to as an optimized Rowland grating (ORG), whose recording sources are aberrated by two auxiliary ORGs. There are two points at which its astigmatism and spherical aberration are canceled in the spectrum of the ORG, therefore the theoretical equations for the mounting are simple. But it is difficult to realize in practical recording because the condition of the ORG is hard to be satisfy.

Sokolova and coworkers[17,18] studied the two-step method which uses a grating objective to generate an aspherical wavefront. But the use of this method is limited to transparent substrates. On the other hand, the theoretical equations are very complicated for the

L. Qing (qingling@mail.ustc.edu.cn) and W. Gang are with the Automation Department, University of Science and Technology of China, Hefei, Anhui 230027, China. L. Bin and W. Qiuping are with the National Synchrotron Radiation Laboratory, University of Science and Technology of China, Hefei, Anhui 230029, China.

Received 10 October 2005; revised 16 January 2006; accepted 30 January 2006; posted 30 January 2006 (Doc. ID 65265).

0003-6935/06/215059-07$15.00/0

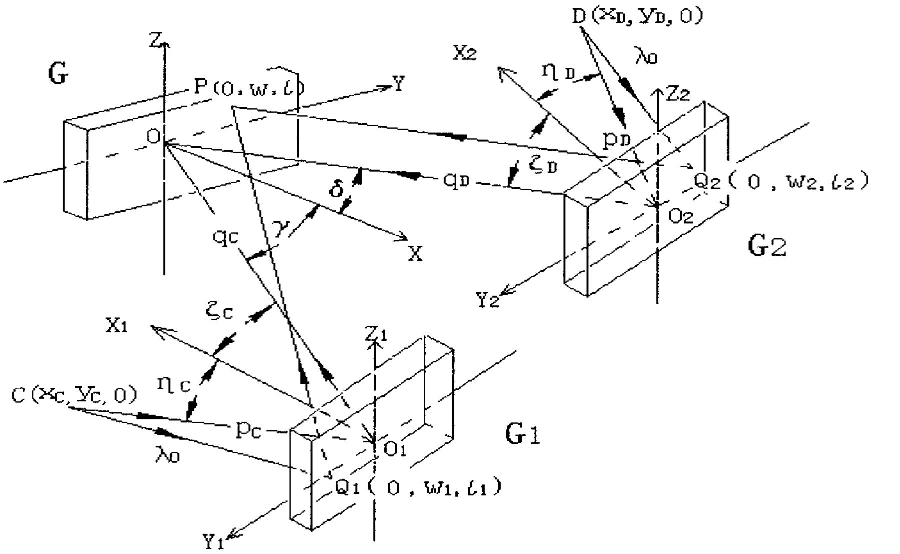

Fig. 1. Schematic diagram of the recording system consists of two coherent point sources, C and D, two uniform line spacing plane gratings, G_1 and G_2, and a plane grating blank G. C, D, G_1, G_2, and G are arranged so that C, D, and the normal of G_1, G_2, and G at their vertices O_1, O_2, and O, lie in a common plane. The incident principal rays CO_1 and DO_2 pass through O after being diffracted at O_1 and O_2, respectively. The distances p_C, q_C, p_D, and q_D, the angles of incidence η_C, γ, η_D, and δ of the principle rays CO_1, O_1O, DO_2, and O_2O, and the angles of diffraction ζ_C and ζ_D of the principle rays O_1O and O_2O are named as recording parameters.

mounting. Therefore the numerical ray-tracing algorithm is applied for the optimal design of recording parameters.

Jobin-Yvon recorded VLS gratings by using auxiliary ULS gratings.[19] But the optimization of the recording parameters was based on numerical ray tracing,[19] which is time consuming and produces the best solutions with difficulty. It is necessary to establish the theoretical equations of groove parameters for the convenience of optimal design.

In this paper the analytical expressions of groove parameters to the fourth order for a recording system where two ULS plane gratings are utilized to generate aspherical wavefronts and a plane blank is regarded as the grating blank are derived. The recording parameters are optimized to record a varied line spacing plane holographic grating with the aid of derived analytical expressions. Section 2 introduces the geometry of recording optics. Section 3 expands the analytical expressions of groove parameters to the fourth order. Section 4 transforms the ray-tracing validation of recording optics to an optimization problem so that it can be solved by a local search method. Section 5 gives an example of a holographic grating recorded in this method and validates the results through the proposed ray-tracing method.

2. Geometry of Recording Optics

The recording optical system is shown in Fig. 1. It consists of two coherent point sources, C and D, two uniform line spacing plane gratings, G_1 and G_2, and a plane grating blank G. C, D, G_1, G_2, and G are arranged so that C, D, and the normal of G_1, G_2, and G at their vertices O_1, O_2, and O lie in a common plane Σ. The incident principal rays CO_1 and DO_2 pass through O after being diffracted at O_1 and O_2, respectively. The distances $p_C = \langle CO_1\rangle$, $q_C = \langle O_1O\rangle$, $p_D = \langle DO_2\rangle$, and $q_D = \langle O_2O\rangle$, the angles of incidence η_C, γ, η_D, and δ of the principle rays CO_1, O_1O, DO_2, and O_2O and the angles of diffraction ζ_C and ζ_D of the principal rays O_1O and O_2O, are called recording parameters.

We introduce two rectangular coordinate systems, one attached to G_1 and the other to G_2. In the $x_1y_1z_1$ (or $x_2y_2z_2$) coordinate system of G_1 (or G_2) the origin is located at O_1 (or O_2), the x_1 (or x_2) axis is the mirror normal at O_1 (or O_2), and the y_1 (or y_2) axis lies in the common plane Σ. Points C and Q_1 on G_1 are designated in the G_1 coordinate system by $C(x_C, y_C, 0)$ and $Q_1(0, w_1, l_1)$. Points D and Q_2 on G_2 are designated in the G_2 coordinate system by $D(x_D, y_D, 0)$ and $Q_2(0, w_2, l_2)$ similarly. Then

$$x_C = p_C \cos \eta_C, \quad x_D = p_D \cos \eta_D,$$

$$y_C = p_C \sin \eta_C, \quad y_D = p_D \sin \eta_D. \tag{1}$$

The sign of η_C (or η_D) is positive or negative according to the way the principal ray, CO_1 (or DO_2) lies in the first or the fourth quadrant of the x_1y_1, (or the x_2y_2) plane in the $x_1y_1z_1$ (or $x_2y_2z_2$) coordinate system.

We introduce an additional rectangular coordinate system xyz attached to the grating blank G. In this system the origin is at O, the x axis is the grating blank normal, and the y axis lies in plane Σ. Points Q_1 on G_1 and Q_2 on G_2 are designated in the G coordinate system by $\bar{Q}_1(\bar{\xi}_1, \bar{w}_1, \bar{l}_1)$ and $\bar{Q}_2(\bar{\xi}_2, \bar{w}_2, \bar{l}_2)$. The sign of γ (or δ) is positive or negative according to the way the principal ray, OO_1 (or OO_2) lies in the first or the fourth quadrant of the xy plane in the xyz coordinate system.

3. Groove Parameters

A ray of wavelength λ_0 originated from C is diffracted at $Q_1(0, w_1, l_1)$ toward point $P(0, w, l)$ on G. Ray DQ_2 of λ_0 travels toward point $P(0, w, l)$ after being diffracted at $Q_2(0, w_2, l_2)$. The groove densities of G_1 and G_2 are $1/\sigma_1$ and $1/\sigma_2$, respectively. According to the grating equation

$$\sin \eta_C + \sin \zeta_C = m_1\lambda_0/\sigma_1, \tag{2a}$$

$$\sin \eta_D + \sin \zeta_D = m_2\lambda_0/\sigma_2, \tag{2b}$$

m_1 (or m_2) is the diffraction order of G_1 (or G_2). The sign of ζ_C (or ζ_D) is positive or negative according to the way the principal ray, O_1O (or O_2O) lies in the first or the fourth quadrant of the x_1y_1 (or x_2y_2) plane in the $x_1y_1z_1$ (or $x_2y_2z_2$) coordinate system.

Then interference fringes are formed on the grating blank G, i.e., the grating grooves, are expressed by

$$\begin{aligned} H = {} & \frac{1}{\lambda_0}\left[(CQ_1 + Q_1P) + w_1m_1\lambda_0/\sigma_1 - (CO_1 + O_1O)\right] \\ & - \frac{1}{\lambda_0}\left[(DQ_2 + Q_2P) + w_2m_2\lambda_0/\sigma_2 - (DO_2 + O_2O)\right]. \end{aligned} \tag{3}$$

Here H is the groove number of point P counted from the zeroth groove that passes through O. H is positive (or negative) when the central point $(0, w_H, 0)$ of the gth groove lies in the first (or fourth) quadrant of the xy plane in the xyz coordinate system.

Substituting Eq. (2) into Eq. (3), and writing Eq. (3) explicitly:

$$H = \frac{1}{\lambda_0}(H_C - H_D), \tag{4a}$$

$$\begin{aligned} H_C = {} & \sqrt{x_C{}^2 = (w_1 - y_C)^2 + l_1{}^2} \\ & + \sqrt{\bar{\xi}_1{}^2 + (\bar{w}_1 - w)^2 + (\bar{l}_1 - l)^2} - (p_C + q_C) \\ & + w_1(\sin \eta_C + \sin \zeta_C), \end{aligned} \tag{4b}$$

$$\begin{aligned} H_D = {} & \sqrt{x_D{}^2 + (w_2 - y_D)^2 + l_2{}^2} \\ & + \sqrt{\bar{\xi}_2{}^2 + (\bar{w}_2 - w)^2 + (\bar{l}_2 - l)^2} - (p_D + q_D) \\ & + w_2(\sin \eta_D + \sin \zeta_D). \end{aligned} \tag{4c}$$

Consider H_C only. Point $\bar{Q}_1(\bar{\xi}_1, \bar{w}_1, \bar{l}_1)$ can be calculated through a coordinate transform from $Q_1(0, w_1, l_1)$:

$$\bar{\xi}_1 = w_1 \sin(-\zeta_C + \gamma) + q_C \cos \gamma,$$

$$\bar{w}_1 = -w_1 \cos(-\zeta_C + \gamma) + q_C \sin \gamma,$$

$$\bar{l}_1 = l_1. \tag{5}$$

Express groove number H in a power series to the fourth order:

$$\begin{aligned} H & = \frac{1}{\lambda_0}\sum_{i=0}^{4}\sum_{j=0}^{4-i} c_{ij}H_{ij}w^i l^j \\ & = \frac{1}{\lambda_0}\sum_{i=0}^{4}\sum_{j=0}^{4-i} c_{ij}(H_{ij})_C w^i l^j - \frac{1}{\lambda_0}\sum_{i=0}^{4}\sum_{j=0}^{4-i} c_{ij}(H_{ij})_D w^i l^j, \end{aligned} \tag{6a}$$

$$H_C = \sum_{i=0}^{4}\sum_{j=0}^{4-i} c_{ij}(H_{ij})_C w^i l^j, \quad H_D = \sum_{i=0}^{4}\sum_{j=0}^{4-i} c_{ij}(H_{ij})_D w^i l^j. \tag{6b}$$

Coefficients c_{ij} are constant. Coefficients H_{ij} are called groove parameters, which are the functions of recording parameters. Consider $(H_{ij})_C$ only. To obtain $(H_{ij})_C$ we must express w_1 and l_1 as the functions of w and l:

$$w_1 = \sum_{i=0}^{4}\sum_{j=0}^{4-i} (A_{ij})_C w^i l^j, \quad l_1 = \sum_{i=0}^{4}\sum_{j=0}^{4-i} (B_{ij})_C w^i l^j. \tag{7}$$

Now we need to calculate the expressions of $(A_{ij})_C$ and $(B_{ij})_C$ with $i + j \le 4$. Applying Fermat's principle to the light path function:

$$\begin{aligned} \text{Min } F_C & = CQ_1 + Q_1P + \sigma_1 w_1 m_1 \lambda_0 \\ & = CQ_1 + Q_1P + w_1(\sin \eta_C + \sin \zeta_C), \end{aligned} \tag{8}$$

yielding the following relationship between direction cosines (L_1, M_1, N_1) of incident ray CQ_1, and the direction cosines $(L_1{}', M_1{}', N_1{}')$ of diffracted ray Q_1P, both defined in the G_1 coordinate system:

$$\begin{aligned} & L_1{}' \\ & = \sqrt{L_1{}^2 - 2(\sin \eta_C + \sin \zeta_C)M_1 - (\sin \eta_C + \sin \zeta_C)^2}, \end{aligned} \tag{9a}$$

$$M_1{}' = M_1 + \sin \eta_C + \sin \zeta_C, \tag{9b}$$

$$N_1{}' = N_1, \tag{9c}$$

where

$$L_1 = -x_C/CQ_1, \quad M_1 = (w_1 - y_C)/CQ_1, \quad N_1 = l_1/CQ_1. \tag{10}$$

The direction cosines (L_C, M_C, N_C) of ray Q_1P in the xyz coordinate system are related to $(L_1{}', M_1{}', N_1{}')$ with simple coordinate transform:

$$L_C = -L_1{}' \cos(-\zeta_C + \gamma) + M_1{}' \sin(\eta_C + \gamma), \tag{11a}$$

$$M_C = -L_1{}' \sin(-\zeta_C + \gamma) + M_1{}' \cos(\eta_C + \gamma), \tag{11b}$$

$$N_C = N_1{}'. \tag{11c}$$

From the definition of direction cosines:

Table 1. Optimized Recording Parameters of Holographic Grating

	γ (rad)	δ (rad)	η_D (rad)	p_c+q_c (mm)	p_D (mm)	q_D (mm)
1	0.0667	0.7010	0.5690	1470.1	461.5	998.5
2	−0.0999	0.4990	1.1427	1326.4	427.8	989.9
3	−0.1748	0.4164	0.9876	1028.0	520.9	380.8
4	−0.0395	0.5690	0.9704	1183.0	601.0	369.8

$$L_C = -\bar{\xi}_1/Q_1P,$$

$$M_C = (w - \bar{w}_1)/Q_1P,$$

$$N_C = (l - \bar{l}_1)/Q_1P. \quad (12)$$

Then

$$w = \bar{w}_1 - \bar{\xi}_1 M_C/L_C, \quad l = \bar{l}_1 - \bar{\xi}_1 N_C/L_C. \quad (13)$$

Substituting Eqs. (1), (5), (7), (8), (10), (11), and (12) into Eq. (13) yields

$$w = f_w[w,\ l,\ (A_{ij})_C,\ (B_{ij})_C,\ \eta_C,\ \zeta_C,\ \gamma,\ p_C,\ q_C], \quad (14a)$$

$$l = f_l[w,\ l,\ (A_{ij})_C,\ (B_{ij})_C,\ \eta_C,\ \zeta_C,\ \gamma,\ p_C,\ q_C], \quad (14b)$$

Expanding Eq. (14) to the fourth order:

$$w = \sum_{i=0}^{4}\sum_{j=0}^{4-i} (f_w)_{ij} w^i l^j, \quad l = \sum_{i=0}^{4}\sum_{j=0}^{4-i} (f_l)_{ij} w^i l^j. \quad (15)$$

$(f_w)_{ij}$ and $(f_l)_{ij}$ are the functions of $(A_{ij})_C$, $(B_{ij})_C$, η_C, ζ_C, γ, p_C, and q_C. By solving equations

$$(f_w)_{ij} = \begin{cases} 1 & i=1,\ j=0 \\ 0 & \text{else} \end{cases}, \quad (f_l)_{ij} = \begin{cases} 1 & i=1,\ j=0 \\ 0 & \text{else} \end{cases}, \quad (16)$$

we can calculate the expressions of $(A_{ij})_C$ and $(B_{ij})_C$ with $i + j \le 4$. Substituting $(A_{ij})_C$ and $(B_{ij})_C$ and Eqs. (5) and (7) into Eq. (4), we can calculate the expressions of $(H_{ij})_C$ as defined in Eq. (6). But it should be noted that the terms of $(A_{ij})_C$ and $(B_{ij})_C$ with $i + j = 3$ and $i + j = 4$ will vanish in the expressions of $(H_{ij})_C$.

The expressions of $(H_{ij})_D$ can be derived similarly. $H_{ij} = (H_{ij})_C - (H_{ij})_D$ in Eq. (6). Rewrite Eq. (6) as

$$H = \frac{1}{\lambda_0}\Big[H_{10}w + \tfrac{1}{2}\left(H_{20}w^2 + H_{02}l^2 + H_{30}w^3 + H_{12}wl^2\right) + \tfrac{1}{8}\left(H_{40}w^4 + 2H_{22}w^2l^2 + H_{04}l^4\right)\Big]. \quad (17)$$

The forms of $(A_{ij})_C$, $(A_{ij})_D$, $(B_{ij})_C$, $(B_{ij})_D$, $(H_{ij})_C$, and $(H_{ij})_D$ are shown in Appendix A.

4. Ray-Tracing Validation Algorithm

In fact, we can obtain H through a numerical method other than analytical expansion. Consider H_C only. Substituting Eqs. (1) and (5) into Eq. (4), H_C is the function of w, l, w_1, l_1, η_C, ζ_C, γ, p_C, and q_C:

$$H_C = f_{H_C}(w,\ l,\ w_1,\ l_1,\ \eta_C,\ \zeta_C,\ \gamma,\ p_C,\ q_C). \quad (18)$$

Given the recording parameters η_C, ζ_C, γ, p_C and q_C, and coordinates w, l of point P on the grating G, H_C is the function of w_1 and l_1. Then

$$H_C = g_{H_C}(w_1,\ l_1). \quad (19)$$

According to Fermat's principle, H_C must be the minimum. H_C can be calculated from the following optimization problem:

$$H_C = \mathrm{Min}\ g_{H_C}(w_1,\ l_1). \quad (20)$$

Applying a local search method with the proper initial value, we can calculate H_C and the corresponding reflecting points $Q_1(0, w_1, l_1)$ for given coordinates w, l of point P on the grating G.

5. Numerical Results

For the VLS plane grating used in a soft x-ray magnetic circular dichroism beamline of the National Synchroton Radiation Laboratory (NSRL), the required groove density is expressed as $n = n_0(1 + b_2w + b_3w^2 + b_4w^3)$, $n_0 = 1400$ (grooves/mm), $b_2 = 8.2453 \times 10^{-4}$(1/mm), $b_3 = 3.0015 \times 10^{-7}$ (1/mm^2), $b_4 = 0.0000 \times 10^{-10}$ (1/mm^3), where

$$n_0 = H_{10}/\lambda_0, \quad b_2 = H_{20}/\lambda_0 n_0,$$

$$b_3 = 3H_{30}/2\lambda_0 n_0, \quad b_4 = H_{40}/2\lambda_0 n_0. \quad (21)$$

The required recording area is 180 mm × 30 mm.

Consider a recording system consisting of an auxiliary plane mirror with a groove density of $1/\sigma_1 = 0$ and an auxiliary uniform line spacing plane grating with a groove density of $1/\sigma_2 = 1000$ grooves/mm. The recording wavelength is $\lambda_0 = 413.1$ mm. The diffrac-

Table 2. Corresponding Groove Density Parameters of Optimization Results

	n_0 (groove/mm)	b_2 (1/mm)	b_3 (1/mm^2)	b_4 (1/mm^3)
1	1.4000×10^3	8.2459×10^{-4}	3.0017×10^{-7}	-2.7332×10^{-14}
2	1.3999×10^3	8.2457×10^{-4}	3.0028×10^{-7}	-5.2081×10^{-14}
3	1.4001×10^3	8.2453×10^{-4}	3.0017×10^{-7}	1.9194×10^{-14}
4	1.3999×10^3	8.2460×10^{-4}	3.0027×10^{-7}	-0.6761×10^{-14}

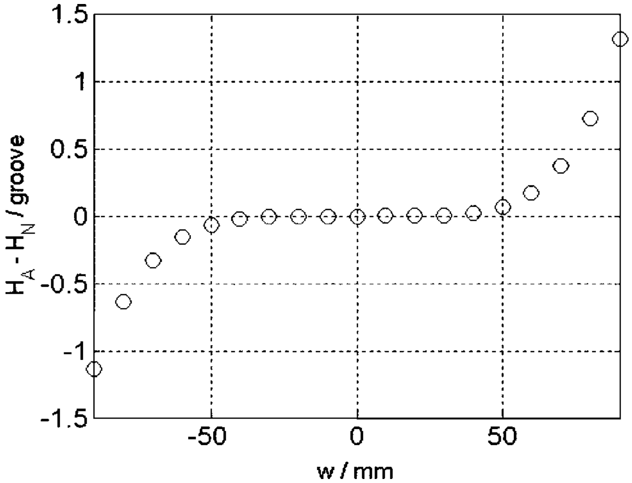

Fig. 2. Groove number error between H_A (computed from analytical expressions) and H_N (computed from exact ray-tracing) l = 0 mm is less than 1.5 lines.

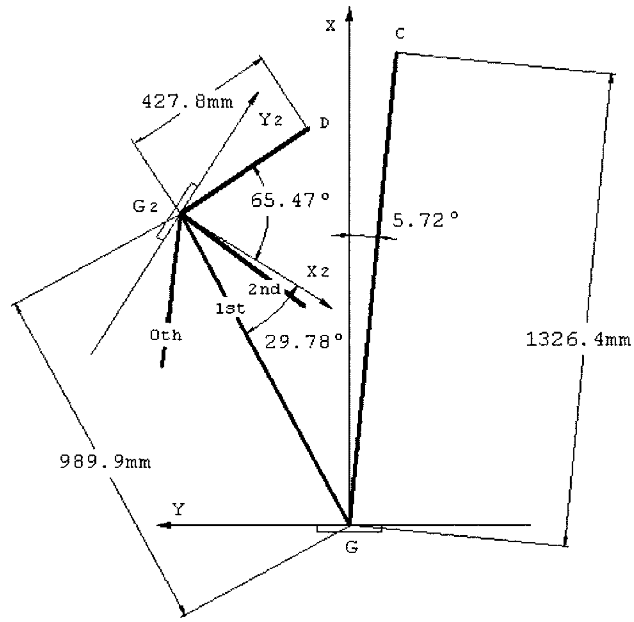

Fig. 3. Two-dimensional schematic recording optics is designed for the varied line spacing holographic grating. Light originating from D is diffracted at auxiliary grating G_2, and the +1 order diffractive light reaches G. Light originating from C reaches G directly because the auxiliary plane mirror can be omitted. It is clear that the other diffractive light will not disturb the recording process when the recording parameters are properly selected.

tion order of the auxiliary grating is +1. Considering the existence of an auxiliary plane mirror, there are six variable recording parameters for optimization: γ, δ, η_D, $p_C + q_C$, p_D, and q_D. η_C, ζ_C, and ζ_D can be calculated according to the relationship of diffraction.

We optimized the recording parameters by using the analytical expressions derived in Appendix A with the evolutionary algorithm.[20] Four groups of optimized recording parameters are shown in Table 1. The corresponding groove density parameters are in Table 2. The theoretical groove density parameters are very close to the required value.

We choose the second group as the practical recording parameters. We checked the design results with the ray-tracing validation algorithm. H_A is the groove number computed from the analytical expressions and H_N is the groove number computed from the ray-tracing validation, at $l = 0$ mm. The error between H_A and H_N is shown in Fig. 2. The ray-tracing results are consistent with those predicted by the theoretical equations. The groove number error, which comes from the truncation error of series expansion, is less than 1.5 lines in the recording area. This proves the exactness of the analytical expressions derived in this paper.

In practical manufacturing, fabrication tolerances are inevitable for any recording parameters, and design results will degrade at that time. Table 3 gives the groove density parameters when the tolerances of distances are 1 mm and the tolerances of angles are 0.001 rad. We can see this mounting is not sensitive to the errors in the recording optics.

The two-dimensional schematic of the recording optics is shown in Fig. 3. The light that originated from D is diffracted at auxiliary grating G_2, and the +1 order diffractive light reaches G. The light that originated from C reaches G directly because the auxiliary plane mirror can be omitted. It is clear that the other diffractive light will not disturb the recording process when the recording parameters are properly selected.

6. Conclusions

Analytical expressions of the groove parameters were derived to the fourth order for recording optics consisting of two uniform line spacing plane auxiliary gratings and a plane grating blank. The derivation of theoretical equations simplifies the optimization of the recording parameters. Based on Fermat's principle and local search, a ray-tracing validation algorithm was provided and proved the exactness of the theoretical equations.

Table 3. Design Results Considering Tolerances for Recording Parameters Group 2

Parameter	Required Value	Design Value
n_0 (groove/mm)	1.4000×10^3	$1.4000 \times 10^3 \pm 0.0047 \times 10^3$
b_2 (1/mm)	8.2453×10^{-4}	$8.2453 \times 10^{-4} \pm 0.0550 \times 10^{-4}$
b_3 (1/mm^2)	3.0015×10^{-7}	$3.0015 \times 10^{-7} \pm 0.0656 \times 10^{-7}$
b_4 (1/mm^3)	0.0000×10^{-10}	$0.0000 \times 10^{-10} \pm 0.0680 \times 10^{-10}$

There are some interesting properties in this mounting:

(i) If the groove densities of two auxiliary gratings are arbitrary, the degree of freedom in this mounting is 10. If the groove densities are fixed, the degree of freedom is 8.

(ii) If the distances p_C and q_C shrink k times simultaneously, the term $(H_{ij})_C$ will expand k^{i+j-1} times. It is the same for $(H_{ij})_D$, p_D, and q_D. This is one reason that this mounting is not sensitive to the tolerances of distance parameters.

(iii) The diffraction area in the auxiliary grating is smaller than the recording area because the diffracted rays are divergent. Therefore groove parameters were not affected heavily by the truncation error of the series expansion in this mounting. On the other hand, in the mounting introduced in Ref. 4, the truncation error is remarkable if the width of the holographic grating to be recorded is too large.

(iv) The recording wavefront is not aberrated in the direction of the auxiliary grating grooves because the grooves are straight. This results in an inability to alter the term H_{02} and H_{04}. Use of varied line spacing or nonplanar auxiliary gratings will solve this problem and will introduce a greater degree of freedom into holographic recording. But apparently it will increase the difficulty in derivation of the analytical expressions and adjustment in practical recording optics.

Appendix A

$$(A_{01})_C = (A_{11})_C = 0, \tag{A1}$$

$$(A_{10})_C = -p_C \cos\gamma \cos\zeta_C / r_C, \tag{A2}$$

$$\begin{aligned}(A_{20})_C = {}& ½(A_{10})^2 \cos^2\eta_C[\cos^2\eta_C(-2q_C \cos\zeta_C \sin\gamma \\ & - q_C \sin\zeta_C \cos\gamma) + \cos^2\zeta_C(-2p_C \cos\zeta_C \\ & \times \sin\gamma + 2p_C \sin\zeta_C \cos\gamma - 3q_C \cos\gamma \\ & \times \sin\eta_C)]/r_C p_C \cos^2\zeta_C \cos\gamma,\end{aligned} \tag{A3}$$

$$(A_{02})_C = -½(B_{01})^2 q_C(\sin\eta_C + \sin\zeta_C)/r_C p_C, \tag{A4}$$

$$(B_{10})_C = (B_{20})_C = (B_{02})_C = 0, \tag{A5}$$

$$(B_{01})_C = 1/p_C(p_C + q_C), \tag{A6}$$

$$\begin{aligned}(B_{11})_C = {}& -(A_{10})_C[r_C \sin\gamma + \cos\zeta_C(q_C \cos\gamma \sin\eta_C \\ & - p_C \sin\zeta_C \cos\gamma)]/\cos\gamma \cos\zeta_C,\end{aligned} \tag{A7}$$

$$(H_{10})_C = -\sin\gamma, \tag{A8}$$

$$\begin{aligned}(H_{20})_C = {}& [(A_{10})_C{}^2 r_C + p \cos\gamma(\cos\gamma \\ & + 2(A_{10})_C \cos\zeta_C)]/p_C q_C,\end{aligned} \tag{A9}$$

$$\begin{aligned}(H_{30})_C = {}& [2(A_{10})_C(A_{20})_C r_C p_C q_C \\ & + (A_{10})_C{}^3(q_C{}^2 \sin\eta_C \cos^2\eta_C \\ & + p_C{}^2 \sin\zeta_C \cos^2\zeta_C) \\ & + (A_{10})_C{}^2 p_C{}^2 \cos\zeta_C(2\cos\gamma \sin\zeta_C \\ & + \sin\gamma \cos\zeta_C) + (A_{10})_C p_C{}^2 \cos\gamma(\cos\gamma \sin\zeta_C \\ & + 2\sin\gamma \cos\zeta_C) + p_C{}^2 \cos\gamma(2q_C(A_{20})_C \cos\zeta_C \\ & + \sin\gamma \cos\gamma)]/p_C{}^2 q_C{}^2,\end{aligned} \tag{A10}$$

$$\begin{aligned}(H_{40})_C = {}& [4(A_{20})_C{}^2 r_C p_C{}^2 q_C{}^2 + 4(A_{10})_C{}^2 p_C{}^3(\cos^2\gamma \\ & + \cos^2\zeta_C) \\ & + 12(A_{10})_C{}^2(A_{20})_C p_C q_C(q_C{}^2 \cos^2\eta_C \sin\eta_C \\ & + p_C{}^2 \cos^2\zeta_C \sin\zeta_C) - 5(A_{10})_C{}^4(q_C{}^3 \cos^4\eta_C \\ & + p_C{}^3 \cos^4\zeta_C) + p_C{}^3 \cos^2\gamma(4 - 5\cos^2\gamma) \\ & + (A_{10})_C{}^3 p_C{}^3 \cos\zeta_C(8\cos\gamma \\ & - 12\cos^2\zeta_C \cos\gamma + 8\sin\gamma \sin\zeta_C \cos\zeta_C) \\ & + (A_{10})_C{}^2 p_C{}^3 \cos\zeta_C \cos\gamma(-14\cos\zeta_C \cos\gamma \\ & + 16\sin\zeta_C \sin\gamma) + (A_{10})_C p_C{}^3 \cos\gamma(8\cos\zeta_C \\ & - 12\cos^2\zeta_C \cos\gamma + 8\sin\gamma \sin\zeta_C \cos\gamma) \\ & + 8(A_{10})_C(A_{20})_C p_C{}^3 q_C \cos\zeta_C(\sin\gamma \\ & + 2\cos\gamma \sin\zeta_C) + 4(A_{10})_C{}^4(q_C{}^3 \cos^2\eta_C \\ & + p_C{}^3 \cos^2\zeta_C) \\ & + 4(A_{20})_C q_C p_C{}^3 \cos\gamma(\cos\gamma \sin\zeta_C \\ & + 2\sin\gamma \cos\zeta_C)]/p_C{}^2 q_C{}^2,\end{aligned} \tag{A11}$$

$$\begin{aligned}(H_{02})_C = {}& [(B_{01})_C{}^2 q_C + (B_{01})_C{}^2 p_C + p_C \\ & - 2(B_{01})_C p_C]/p_C q_C,\end{aligned} \tag{A12}$$

$$\begin{aligned}(H_{12})_C = {}& \{(A_{10})_C(B_{01})_C{}^2(p_C{}^2 \sin\zeta_C + q_C{}^2 \sin\eta_C) \\ & + 2(B_{10})_C(B_{11})_C p_C q_C(p_C + q_C) \\ & + (A_{10})_C p_C{}^2 \sin\zeta_C(1 - 2(B_{01})_C) \\ & + (B_{01})_C p_C{}^2 \sin\gamma[(B_{01})_C - 2] \\ & + 2(A_{10})_C(A_{02})_C r_C p_C q_C - 2(B_{11})_C p_C{}^2 q_C \\ & + p_C{}^2 \sin\gamma \\ & + 2(A_{02})_C p_C{}^2 q_C \cos\gamma \cos\zeta_C\}/p_C{}^2 q_C{}^2,\end{aligned} \tag{A13}$$

$$\begin{aligned}(H_{22})_C = {}& p_C{}^3(2 - 4(B_{01})_C + 2(B_{01})_C{}^2 + 2(A_{10})_C{}^2 \\ & - 3\cos^2\gamma) + 2(B_{11})_C{}^2 p_C{}^2 q_C{}^2(p_C + q_C) \\ & - 3(A_{10})_C{}^2(B_{01})_C{}^2(q_C{}^3 \cos^2\eta_C + p_C{}^3 \cos^2\zeta_C) \\ & + 4(A_{10})_C(B_{01})_C p_C{}^3(\cos\zeta_C \cos\gamma \\ & - 2\sin\zeta_C \sin\gamma) \\ & - 2(A_{10})_C(B_{01})_C{}^2 p_C{}^3(\cos\zeta_C \cos\gamma \\ & - 2\sin\zeta_C \sin\gamma) + 4(B_{11})_C p_C{}^3 q_C \sin\gamma[(B_{01})_C \\ & - 1] - 2(A_{10})_C p_C{}^3(\cos\zeta_C \cos\gamma \\ & - 2\sin\zeta_C \sin\gamma) + 2(A_{10})_C{}^2(B_{01})_C{}^2(p_C{}^3 + q_C{}^3) \\ & + 4(A_{10})_C(B_{01})_C(B_{11})_C p_C q_C(p_C{}^2 \sin\zeta_C \\ & + q_C{}^2 \sin\eta_C) - 3(A_{10})_C{}^2 p_C{}^3 \cos^2\zeta_C\end{aligned}$$

$$
\begin{aligned}
&+2(A_{10})_C{}^2(B_{01})_C p_C{}^3(3\cos^2\zeta_C-2)\\
&-4(A_{10})_C(B_{11})_C p_C{}^3 q_C\sin\zeta_C\\
&+6(A_{10})_C{}^2(A_{02})_C p_C q_C\big(p_C{}^2\cos^2\zeta_C\sin\zeta_C\\
&+q_C{}^2\cos^2\eta_C\sin\eta_C\big)\\
&+4(A_{10})_C(A_{02})_C p_C{}^3 q_C\cos\zeta_C(2\cos\gamma\sin\zeta_C\\
&+\sin\gamma\cos\zeta_C)+4(A_{20})_C(A_{02})_C r_C(p_C+q_C)\\
&+2(A_{20})_C(B_{01})_C{}^2 p_C q_C\big(p_C{}^2\sin\zeta_C+q_C{}^2\sin\eta_C\big)\\
&+2(A_{02})_C p_C{}^3 q_C\cos\gamma(\cos\gamma\sin\zeta_C+2\sin\gamma\cos\zeta_C)\\
&+3(B_{01})_C p_C{}^3\cos^2\gamma[2-(B_{01})_C]\\
&+2(A_{20})_C p_C{}^3 q_C\sin\zeta_C(1-2(B_{01})_C)/p_C{}^3 q_C{}^3, \qquad \text{(A14)}
\end{aligned}
$$

$$
\begin{aligned}
(H_{04})_C=\big[&p_C{}^3(-1+4(B_{01})_C-6(B_{01})_C{}^2+4(B_{01})_C{}^3)\\
&-(B_{01})_C{}^4\big(p_C{}^3+q_C{}^3\big)\\
&+4(A_{02})_C(B_{01})_C{}^2 p_C q_C\big(p_C{}^2\sin\zeta_C\\
&+q_C{}^2\sin\eta_C\big)+4(A_{02})_C{}^2 r_C p_C q_C\\
&+4(A_{02})_C p_C{}^3 q_C\sin\zeta_C(1-2(B_{01})_C)\big]/p_C{}^3 q_C{}^3,
\end{aligned}
\qquad \text{(A15)}
$$

where

$$
r_C=q_C\cos^2\eta_C+p_C\cos^2\zeta_C. \qquad \text{(A16)}
$$

For the expression $(A_{ij})_D$, $(B_{ij})_D$, and $(H_{ij})_D$, change η_C, ζ_C, γ, p_C, q_C, and r_C to η_D, ζ_D, δ, p_D, q_D, and r_D.

References

1. T. Namioka, M. Seya, and H. Noda, "Design and performance of holographic concave gratings," Jpn. J. Appl. Phys. **15,** 1181–1197 (1976).
2. M. Koike and Y. Harada, "New blazed holographic grating fabricated by using an aspherical recording with an ion-etching method," Proc. SPIE **815,** 96–101 (1987).
3. M. Duban, "Holographic aspheric gratings printed with aberrant waves," Appl. Opt. **26,** 4263–4273 (1987).
4. T. Namioka and M. Koike, "Aspheric wave-front recording optics for holographic gratings," Appl. Opt. **34,** 2180–2186 (1995).
5. H. Noda, Y. Harada, and M. Koike, "Holographic grating recorded using aspheric wavefronts for a Seya–Namioka monochromator," Appl. Opt. **28,** 4375–4380 (1989).
6. M. Koike and T. Namioka, "Optimization and evaluation of varied line spacing plane grating monochromators for third generation synchrotron radiation sources," J. Electron Spectrosc. Relat. Phenom. **80,** 303–308 (1996).
7. K. Amemiya, Y. Kitajima, Y. Yonamoto, T. Ohata, K. Ito, K. Sano, T. Nagano, M. Koeda, H. Sasai, and Y. Harada, "Fabrication of a varied-line-spacing plane grating with aspheric wavefront holographic recording for a new grazing incidence monochromator at Photon Factory," Proc. SPIE **3150,** 171–182 (1997).
8. M. Koike, T. Yamazaki, and Y. Harada, "Design of holographic gratings recorded with aspheric wavefront recording optics for soft x-ray flat-field spectrographs," J. Electron Spectrosc. Relat. Phenom. **101,** 913–918 (1999).
9. M. Duban, "Third-generation Rowland holographic mounting," Appl. Opt. **30,** 4019–4025 (1991).
10. M. Duban, "Theory of spherical holographic gratings recorded by use of a multimode deformable mirror," Appl. Opt. **37,** 7209–7213 (1998).
11. M. Duban, "Recording high-dispersion spherical holographic gratings in a modified Rowland mounting by use of a multimode deformable mirror," Appl. Opt. **39,** 16–19 (2000).
12. M. Duban, G. Lemaitre, and R. Malina, "Recording method for obtaining high-resolution holographic gratings through use of multimode deformable plane mirrors," Appl. Opt. **37,** 3438–3439 (1998).
13. M. Duban, K. Dohlen, and G. Lemaitre, "Illustration of the use of multimode deformable plane mirrors to record high-resolution concave gratings: results for the Cosmic Origins Spectrograph gratings of the Hubble Space Telescope," Appl. Opt. **37,** 7214–7217 (1998).
14. G. Lemaitre and M. Duban, "Corrected grating recording by active optics compensator case of HST Cosmic Origins Spectrometer," Proc. SPIE **4854,** 447–456 (2003).
15. M. Duban, "Third-generation Rowland holographic mounting: fourth-order theory," Appl. Opt. **38,** 3443–3449 (1999).
16. M. Duban, "High-dispersion spherical holographic gratings in a modified Rowland mounting," Appl. Opt. **40,** 1599–1608 (2001).
17. E. Sokolova, "Geometric theory of two-steps recorded holographic diffraction gratings," Proc. SPIE **3450,** 113–124 (1998).
18. E. Sokolova, B. Kruizinga, and I. Golubenko, "Recording of concave diffraction gratings in a two-step process using spatially incoherent light," Opt. Eng. **43,** 2613–2622 (2004).
19. B. Deville, F. Bonnemason, J. Flamand, V. Millet, A. Thevenon, V. Gattino, and B. Touzet, "Holographically recorded, ion etched variable line space gratings," Proc. SPIE **3450,** 24–35 (1998).
20. Q. Ling, G. Wu, and Q. Wang, "Restricted evolution based multimodal function optimization in holographic grating design," in *Proceedings of IEEE Congress on Evolutionary Computation* (IEEE, 2005), pp. 789–794.